

See discussions, stats, and author profiles for this publication at: <https://www.researchgate.net/publication/44631769>

Two-Phase Thermodynamic Model for Efficient and Accurate Absolute Entropy of Water from Molecular Dynamics Simulations

Article in *The Journal of Physical Chemistry B* · June 2010

DOI: 10.1021/jp103120q · Source: PubMed

CITATIONS
323

READS
2,182

3 authors:



Shiang-Tai Lin

National Taiwan University

187 PUBLICATIONS 6,790 CITATIONS

[SEE PROFILE](#)



Prabal K Maiti

Indian Institute of Science Bangalore

317 PUBLICATIONS 8,402 CITATIONS

[SEE PROFILE](#)



William A. Goddard

California Institute of Technology

2,188 PUBLICATIONS 173,184 CITATIONS

[SEE PROFILE](#)

Two-Phase Thermodynamic Model for Efficient and Accurate Absolute Entropy of Water from Molecular Dynamics Simulations

Shiang-Tai Lin,*† Prabal K. Maiti,‡ and William A. Goddard III§

Department of Chemical Engineering, National Taiwan University, Taipei 10617, Taiwan, Centre for Condensed Matter Theory, Department of Physics, Indian Institute of Science, Bangalore 560012, India, and Materials and Process Simulation Center, Beckman Institute, California Institute of Technology, Pasadena, California 91125

Received: April 7, 2010; Revised Manuscript Received: May 14, 2010

Presented here is the two-phase thermodynamic (2PT) model for the calculation of energy and entropy of molecular fluids from the trajectory of molecular dynamics (MD) simulations. In this method, the density of state (DoS) functions (including the normal modes of translation, rotation, and intramolecular vibration motions) are determined from the Fourier transform of the corresponding velocity autocorrelation functions. A fluidicity parameter (f), extracted from the thermodynamic state of the system derived from the same MD, is used to partition the translation and rotation modes into a diffusive, gas-like component (with $3Nf$ degrees of freedom) and a nondiffusive, solid-like component. The thermodynamic properties, including the absolute value of entropy, are then obtained by applying quantum statistics to the solid component and applying hard sphere/rigid rotor thermodynamics to the gas component. The 2PT method produces exact thermodynamic properties of the system in two limiting states: the nondiffusive solid state (where the fluidicity is zero) and the ideal gas state (where the fluidicity becomes unity). We examine the 2PT entropy for various water models (F3C, SPC, SPC/E, TIP3P, and TIP4P-Ew) at ambient conditions and find good agreement with literature results obtained based on other simulation techniques. We also validate the entropy of water in the liquid and vapor phases along the vapor–liquid equilibrium curve from the triple point to the critical point. We show that this method produces converged liquid phase entropy in tens of picoseconds, making it an efficient means for extracting thermodynamic properties from MD simulations.

1. Introduction

The thermodynamic properties of water (especially the energy and entropy) provide valuable insights into its role in various biological processes^{1,2} (protein folding, ligand binding, etc.). There has been growing interest in the evaluation of absolute entropy of water, and several methods are proposed to determine the entropy of water from the results of molecular dynamics simulations. For example, White and Meirovitch^{3,4} proposed a hypothetical scanning method which determines the absolute entropy and free energy from the Boltzmann probability distribution. Lizaridis and Karplus⁵ showed that the entropy can be obtained from truncated expansion of molecular pair correlation functions.⁶ More recently, Sharma et al.⁷ report the accuracy of entropy determined from the two-body pair correlation function determined from atom–atom radial distribution functions. Tyka et al.⁸ proposed a confinement method that determines the absolute entropy using thermodynamic integration from a hypothetical harmonic state to the liquid state. Henchman⁹ demonstrated estimation of entropy from cell theory, in which the entropy is calculated within the harmonic approximation in the potential surface. These methods have been applied to water but only under limited conditions (e.g., at 1 atm and 25 °C). Furthermore, the harmonic approximations implicit in some of these methods make the results suspect since anharmonic effects are known to be important in diffusive systems.^{10,11} It is thus questionable whether these methods would

be applicable to study the properties of water under various physical and chemical environments around biological molecules.¹²

Recently, Lin et al.¹¹ developed the two-phase thermodynamic (2PT) model that determines the thermodynamic properties of a system from its density of state (DoS) function (the Fourier transform of the velocity autocorrelation function) by separating out the diffusional contributions from the vibrational contributions. This separation is critical since the DoS is generally finite for zero frequency (being proportional to the diffusion constant) so that blind application of the quantum statistical formulas for vibration would lead to infinite entropy. The DoS function provides information about the normal mode distribution of the system and about diffusion. Thus, the zero frequency intensity in the DoS is proportional to the diffusivity of the system.¹³ For solids, the DoS function represents the phonon spectrum as in the Debye–Einstein model.¹⁴ This allows thermodynamic properties to be obtained by treating the system as a continuous collection of noninteracting quantum harmonic oscillators. For gases, the DoS decays exponentially with frequency so that such harmonic approximations are not valid, but the classical theory for gases can be used to determine the thermodynamic properties. Lin et al.¹¹ observed that the DoS of fluids possesses the key features of both the gas and the solid. A fluidicity parameter, f , was derived to determine the weights of the gas-like and the solid-like components in any system. Applying the proper theories to each DoS component, they showed that accurate thermodynamic properties (with quantum corrections) of monoatomic gases can be obtained over the whole phase diagram (gas, liquid, and solid), leading to excellent quantitative agreement with the results of a very accurate equation of state in all regions

* To whom correspondence should be addressed. E-mail: stlin@ntu.edu.tw.

† National Taiwan University.

‡ Indian Institute of Science.

§ California Institute of Technology.

(gas, liquid, solid, supercritical, and even in the metastable and unstable regions).

In this work, we extend the 2PT model to molecular systems, showing that the rotational DoS may also be considered as the superposition of that of free (gas) and hindered (solid) rotors. Therefore, rotational contributions to the thermodynamic properties can be obtained in a way similar to the translational motions. We validate this idea with water whose thermodynamic properties are known accurately over a large range of temperature and pressure conditions (e.g., steam tables). We find that 2PT provides very accurate values of energy and entropy from a short (~ 10 ps) molecular dynamics simulations.

2. Theory

2.1. Density of State Function. The density of state function, $S(v)$, is defined as the mass weighted sum of the atomic spectral densities^{11,13}

$$S(v) = \frac{2}{kT} \sum_{j=1}^N \sum_{k=1}^3 m_j s_j^k(v) \quad (1)$$

where m_j is the mass of atom j and N is the total number of atoms of the system. The spectral density $s_j^k(v)$ of atom j in the k direction ($k = x, y$, and z in the Cartesian coordinate) is determined from the square of the Fourier transform of the velocities as

$$s_j^k(v) = \lim_{\tau \rightarrow \infty} \frac{1}{2\tau} \left| \int_{-\tau}^{\tau} v_j^k(t) e^{-i2\pi vt} dt \right|^2 \quad (2)$$

where $v_j^k(t)$ is the k -component of the velocity vector of atom j at time t . The atom spectral density and the density of state function may also be obtained from the Fourier transform of the velocity autocorrelation function.^{11,13}

The physical significance of $S(v)$ is that it represents the density of normal modes of the system at frequency v

$$S(v) = \sum_{i=1}^{3N} [\delta(v - v_i^n) + \delta(v + v_i^n)] \quad (3)$$

where v_i^n represents the i th of the $3N$ normal-mode frequencies of the system. In other words, $S(v)dv$ is the number of modes of a system moving within the frequency range of v to $v + dv$. Therefore, the integration of $S(v)$ gives the total degrees of freedom of the system, i.e.

$$\int_0^\infty S(v)dv = 3N \quad (4)$$

Furthermore, the intensity of $S(v)$ at zero frequency is associated with the diffusivity D of the particles^{11,13}

$$S(0) = \frac{12mND}{kT} \quad (5)$$

2.2. Two-Phase Thermodynamic Model (2PT) for Thermodynamic Properties. **2.2.1. Thermodynamic Properties of Systems Undergo Harmonic Motions.** For solid state systems (e.g., crystals), where all the normal modes are essentially harmonic, the canonical partition function, Q , can be determined

as the product of those of harmonic oscillators ($q_{HO}(v)$) having the same vibration frequencies, i.e.

$$\ln Q = \int_0^\infty dv S(v) \ln q_{HO}(v) \quad (6)$$

where $q_{HO}(v) = (\exp(-\beta hv/2))/(1 - \exp(-\beta hv/2))$ with $\beta = 1/kT$ and h being the Plank constant. The thermodynamic properties of such systems can be expressed in terms of the integration of the density of state function weighted by the corresponding property weighting functions^{11,13}

$$E = E_0 + T\beta^{-1} \left(\frac{\partial \ln Q}{\partial T} \right)_{N,V} = E_0 + \beta^{-1} \int_0^\infty dv S(v) W_E(v) \quad (7a)$$

$$S = k \ln Q + \beta^{-1} \left(\frac{\partial \ln Q}{\partial T} \right)_{N,V} = k \int_0^\infty dv S(v) W_S(v) \quad (7b)$$

$$A = E_0 - \beta^{-1} \ln Q = E_0 + \beta^{-1} \int_0^\infty dv S(v) W_A(v) \quad (7c)$$

where the energy, entropy, and Helmholtz free energy weighting functions are

$$W_E(v) = \frac{\beta hv}{2} + \frac{\beta hv}{\exp(\beta hv) - 1} \quad (8a)$$

$$W_S(v) = \frac{\beta hv}{\exp(\beta hv) - 1} - \ln[1 - \exp(-\beta hv)] \quad (8b)$$

$$W_A(v) = \ln \frac{1 - \exp(\beta hv)}{\exp(-\beta hv/2)} \quad (8c)$$

The reference energy E_0 is the potential energy of the system at 0 K. For convenience, we choose to subtract the kinetic energy from the total energy (e.g., E^{MD} in a molecular dynamic simulation) as

$$E_0 = E^{\text{MD}} - \beta^{-1} 3N \quad (9)$$

Equation 9 ensures that the total energy E (eq 7a) determined from a classical MD simulation is the same as the sum of energies of classical harmonic oscillators ($q_{HO}^C(v) = (1/(\beta hv))$ standing still).¹¹

The set of equations presented in this section are also referred to as the one-phase thermodynamic (1PT) model.

2.2.2. Thermodynamic Properties of Monatomic Fluids. The DoS of monatomic gases and liquids represents the translational motions of the molecules. The low frequency modes (diffusive motions and libration), which are highly anharmonic, dominate the properties of the system; therefore, eqs 7a to 9 are no longer valid. Lin et al. resolved this problem by treating the density of states of a fluidic system as the sum of a gas-like ($S^g(v)$) and a solid-like ($S^s(v)$) contribution¹¹

$$S(v) = S^g(v) + S^s(v) \quad (10)$$

where $S^g(v)$ accounts for all the diffusive components (i.e., $S(v = 0) = S^g(v = 0) = s_{\text{trn}}^0$), and the solid component is nondiffusive ($S^s(0) = 0$). The density of states of the gas-like component is assumed to be that of hard spheres¹¹

$$S^g(v) = \frac{s_{\text{trn}}^0}{1 + \left[\frac{\pi s_{\text{trn}}^0 v}{6 f_{\text{trn}} N} \right]^2} \quad (11)$$

where $s_{\text{trn}}^0 = S(0)$ is the intensity of the density of state of the real system at zero frequency. The variable f_{trn} indicates the translational fluidicity of the system (total degrees of freedom of the gas-like component is $\int_0^\infty S^g(v) dv = 3Nf_{\text{trn}}$). In the high-temperature and/or low density limit where the fluid is nearly a gas of hard spheres, the value of f_{trn} should be unity. In the high density limit where the system is a solid, f_{trn} should be zero. Lin et al.¹¹ suggested that these limiting values can be met by setting the value of f_{trn} to be the ratio of the diffusivity of the system to that of a hard sphere gas under the same temperature and density. A universal equation can thus be derived for the fluidicity as (readers are referred to ref 11 for derivation details)

$$2\Delta^{-9/2}f^{15/2} - 6\Delta^{-3}f^5 - \Delta^{-3/2}f^{7/2} + 6\Delta^{-3/2}f^{5/2} + 2f - 2 = 0 \quad (12)$$

where $f = f_{\text{trn}}$ for the translational contributions, and the dimensionless diffusivity constant Δ is a function of material properties

$$\Delta(T, V, N, m, s^0) = \frac{2s^0}{9N} \left(\frac{\pi k T}{m} \right)^{1/2} \left(\frac{N}{V} \right)^{1/3} \left(\frac{6}{\pi} \right)^{2/3} \quad (13)$$

where V is the volume of the system. [Note that $f = f_{\text{trn}}$ (in eq 12) and $s^0 = s_{\text{trn}}^0$ (in eq 13) for translational motions.] Therefore, the thermodynamic state (N, V, T) of the system and the diffusivity (s^0) obtained from MD simulation uniquely determine the value of Δ (eq 13) and thus the fluidicity f_{trn} (eq 12) and $S^g(v)$. The value of f increases monotonically with increasing Δ (see Figure 2 in ref 11). For small values of Δ ($< 10^{-4}$), the last two terms on the right side of eq 12 dominate, and thus $f \rightarrow 1$. For large values of Δ ($> 10^2$), the first term dominates and $f \rightarrow 0$.

With this 2PT decomposition of the density of states, the thermodynamic properties of the system are determined as the sum of the gas and solid contributions

$$E = E_0 + \beta^{-1} \left[\int_0^\infty dv S^s(v) W_E^s(v) + \int_0^\infty dv S^g(v) W_E^g(v) \right] \quad (14a)$$

$$S = k \left[\int_0^\infty dv S^s(v) W_S^s(v) + \int_0^\infty dv S^g(v) W_S^g(v) \right] \quad (14b)$$

$$A = E_0 + \beta^{-1} \left[\int_0^\infty dv S^s(v) W_A^s(v) + \int_0^\infty dv S^g(v) W_A^g(v) \right] \quad (14c)$$

where the weighting functions for the solid-like component ($W_E^s(v)$, $W_S^s(v)$, and $W_A^s(v)$) are the same as those in eq 8a, and those for the gas-like component are

$$W_E^g(v) = W_S^g(v) = W_A^g(v) = 0.5 \quad (15a)$$

$$W_S^g(v) = W_A^g(v) = \frac{1}{3} \frac{S^{\text{HS}}}{k} \quad (15b)$$

$$W_A^g(v) = W_A^{\text{HS}}(v) = W_E^{\text{HS}}(v) - W_S^{\text{HS}}(v) \quad (15c)$$

where S^{HS} is the hard sphere entropy

$$\frac{S^{\text{HS}}(f_{\text{trn}} N, V, T)}{k} = \frac{5}{2} + \ln \left[\left(\frac{2\pi m k T}{h^2} \right)^{3/2} \frac{V}{f_{\text{trn}} N} z(y) \right] + \frac{y(3y - 4)}{(1 - y)^2} \quad (16)$$

and $y = (f_{\text{trn}}^{5/2})/(\Delta^{3/2})$. $z(y)$ is the compressibility factor from the Carnahan–Starling equation of state of hard sphere gases

$$z(y) = \frac{1 + y + y^2 - y^3}{(1 - y)^3} \quad (17)$$

The reference energy now becomes

$$E_0 = E^{\text{MD}} - \beta^{-1} 3N(1 - 0.5f_{\text{trn}}) \quad (18)$$

Equations 10–18 constitute the 2PT method for obtaining thermodynamic properties of monatomic fluids (e.g., argons) based on the density of state distribution.^{1,11,15,16}

2.2.3. Thermodynamic Properties of Polyatomic Fluids. For polyatomic species (e.g., water), it is possible to decompose the total density of state functions into contributions from molecular translation ($S_{\text{trn}}(v)$), rotation ($S_{\text{rot}}(v)$), and vibration ($S_{\text{vib}}(v)$)

$$S(v) = S_{\text{trn}}(v) + S_{\text{rot}}(v) + S_{\text{vib}}(v) \quad (19)$$

where the $S_{\text{trn}}(v)$ is determined from the center of mass velocities of all the molecules, and $S_{\text{vib}}(v)$ is determined from intramolecular vibration velocities. The rotational density of state is determined from the angular velocity (analogous to eqs 1 and 2)

$$S_{\text{rot}}(v) = \beta \sum_{l=1}^M \sum_{k=1}^3 \lim_{\tau \rightarrow \infty} \frac{I_l^k}{\tau} \left| \int_{-\tau}^{\tau} \omega_l^k(t) e^{-i2\pi v t} dt \right|^2 \quad (20)$$

where I_l^k is the k -th principle moment of inertia of molecule l ; ω_l^k is the angular velocity along the k principal axis; and M is the total number of molecules in the system.

In analogy to the gas–solid decomposition for the translational spectrum (eq 10), the anharmonic effect in rotational motions can be treated by decomposing the rotational density of state into a gas and a solid-like component

$$S_{\text{rot}}(v) = S_{\text{rot}}^g(v) + S_{\text{rot}}^s(v) \quad (21)$$

with the gas component being determined as

$$S_{\text{rot}}^g(v) = \frac{s_{\text{rot}}^0}{1 + \left[\frac{\pi s_{\text{rot}}^0 v}{6 f_{\text{rot}} N} \right]^2} \quad (22)$$

with $s_{\text{rot}}^0 = S_{\text{rot}}(v = 0)$ so that all the rotational diffusional behavior is considered in the gas component and the rotational fluidicity f_{rot} is determined from eqs 12 and 13 with $s^0 = s_{\text{rot}}^0$. Therefore, the value of $S_{\text{rot}}(0)$ and f_{rot} uniquely determines $S_{\text{rot}}^g(v)$ and thus $S_{\text{rot}}^s(v)$.

The thermodynamic properties of molecular fluids are determined as a sum of contributions from the corresponding translation, rotation, and vibration motions

$$E = E_0 + E_{\text{trn}} + E_{\text{rot}} + E_{\text{vib}} \quad (23a)$$

$$S = S_{\text{trn}} + S_{\text{rot}} + S_{\text{vib}} \quad (23b)$$

$$A = E_0 + A_{\text{trn}} + A_{\text{rot}} + A_{\text{vib}} \quad (23c)$$

and the properties associated with each type of motions determined from the corresponding density of state functions

$$E_m = \beta^{-1} \left[\int_0^\infty dv S_m^s(v) W_{m,E}^s(v) + \int_0^\infty dv S_m^g(v) W_{m,E}^g(v) \right] \quad (24a)$$

$$S_m = k \left[\int_0^\infty dv S_m^s(v) W_{m,S}^s(v) + \int_0^\infty dv S_m^g(v) W_{m,S}^g(v) \right] \quad (24b)$$

$$A_m = \beta^{-1} \left[\int_0^\infty dv S_m^s(v) W_{m,A}^s(v) + \int_0^\infty dv S_m^g(v) W_{m,A}^g(v) \right] \quad (24c)$$

where $m = \text{trn}$ (center of mass translation), rot (rotation), or vib (intramolecular vibration). For vibration motions ($m = \text{vib}$), the gas component is always zero, $S_{\text{vib}}^g(v) = 0$; i.e., all vibrational motions are taken as harmonic, $S_{\text{vib}}(v) = S_{\text{vib}}^s(v)$.

The harmonic weighting functions (eq 8a) are used for all solid components ($W_{m,E}^s(v)$, $W_{m,S}^s(v)$, and $W_{m,A}^s(v)$). The hard sphere weighting functions (eq 15a) are used for the gas-like component of the translational motions ($W_{\text{trn},E}^g(v)$, $W_{\text{trn},S}^g(v)$, and $W_{\text{trn},A}^g(v)$). The ideal gas weighting functions are used for the gas-like component of rotational motions

$$W_{\text{rot},E}^g(v) = 0.5 \quad (25a)$$

$$W_{\text{rot},S}^g(v) = \frac{1}{3} \frac{S^R}{k} \quad (25b)$$

$$W_{\text{rot},A}^g(v) = W_{\text{rot},E}^g(v) - W_{\text{rot},S}^g(v) \quad (25c)$$

where $(S^R/k) = \ln\{[(\pi^{1/2}e^{3/2})/(\sigma)](T^3/(\Theta_A\Theta_B\Theta_C))^{1/2}\}$ is the rotational entropy of a rigid body with rotational temperatures $\Theta_A = h^2/(8\pi^2 I_A k)$ and σ is the rotational symmetry. The reference potential energy is taken to be

$$E_0 = E^{\text{MD}} - \beta^{-1} 3N(1 - 0.5f_{\text{trn}} - 0.5f_{\text{rot}}) \quad (26)$$

It should be noted that the 2PT method provides the correct thermodynamic properties in the limits of (1) crystalline solid where the molecular diffusivity is zero (and hence $f_{\text{trn}} = f_{\text{rot}} = 0$, and the system possesses only solid-like component) and (2) ideal gas where the fluidicity f_{trn} and f_{rot} are unity. We will demonstrate that this method does provide reliable values of thermodynamic properties of water for conditions between these two limits.

3. Computational Details

The entropy of water along the vapor–liquid saturation curve is examined using five water models, F3C,¹⁷ TIP3P,¹⁸ TIP4P-Ew,¹⁹ SPC,²⁰ and SPC/E.²¹ We use a 3-dimensional periodic unit cell containing 512 water molecules at desired densities. We took the temperature and density of the vapor and liquid phases from the steam table.²² Open source package LAMMPS²³ was used for all constant volume, temperature, and number of particle (NVT) molecular dynamics simulations. At each temperature and density, the system was first equilibrated for 1–2 ns followed by 100 ps to 1 ns NVT simulations for entropy calculations. Long-range interactions were included using the particle–particle particle–mesh Ewald method²⁴ (with a precision of 4.18×10^{-5} kJ/mol), and the Nose–Hoover thermostat²⁵ was used to control the temperature (with the relaxation time set to 0.1 ps). The integration time step was set to 1 fs, and the simulation trajectory (energy, atomic coordinates, and velocities) was recorded every 4 fs. We used a cutoff value for van der Waals interaction of 9.5 Å and for real-space Ewald of 8.5 Å.

To determine the density of state function for the three types of motions, the atomic velocity was decomposed into translation, rotation, and vibration components at every step, i.e.

$$\vec{v}_j^k(t) = \vec{v}_{j,\text{trn}}^k(t) + \vec{v}_{j,\text{rot}}^k(t) + \vec{v}_{j,\text{vib}}^k(t) \quad (27)$$

The translational velocity ($\vec{v}_{j,\text{trn}}$) on atom j is set to be the center of mass velocity of the molecule to which the atom belongs. The angular velocity ($\vec{\omega}$) is determined from the angular momentum (\vec{L}) and the (inverse of) principle moments of inertia tensor (\mathbf{I})

$$\vec{L} = \sum m_j \vec{r}_j \times \vec{v}_j = \mathbf{I} \vec{\omega} \quad (28)$$

where \vec{r}_j is the position vector of atom j to the center of mass of the molecule, and the summation is over all the atoms in the molecule. The rotational velocity is then obtained from $\vec{v}_j^{\text{rot}} = \vec{\omega} \times \vec{r}_j$ and the vibrational velocity from $\vec{v}_{j,\text{vib}} = \vec{v}_j - \vec{v}_{j,\text{trn}} - \vec{v}_{j,\text{rot}}$. Once the velocity components are determined, the density of state functions $S_m(v)$ are calculated from eq 1 (for $m = \text{trn}$ and vib) and eq 20 (for $m = \text{rot}$).

To determine thermodynamic properties using the 2PT model, the constants Δ are first calculated from eq 13 for the translation (where $s^0 = S_{\text{trn}}(0)$) and rotation (where $s^0 = S_{\text{rot}}(0)$), respectively. The corresponding fluidicity factors f_{trn} and f_{rot} were then solved from eq 14a (using Newton's method). Having $S_{\text{trn}}(0)$ and f_{trn} , the DoS of the gas component $S_{\text{trn}}^g(v)$ is completely determined (eq 11). The solid component $S_{\text{trn}}^s(v)$ is obtained by subtracting $S_{\text{trn}}^g(v)$ from the total $S_{\text{trn}}(v)$ of the real system. Similarly, $S_{\text{rot}}(0)$ and f_{rot} completely determine $S_{\text{rot}}^g(v)$ (eq 22) and thus $S_{\text{rot}}^s(v)$. The thermodynamic properties are then

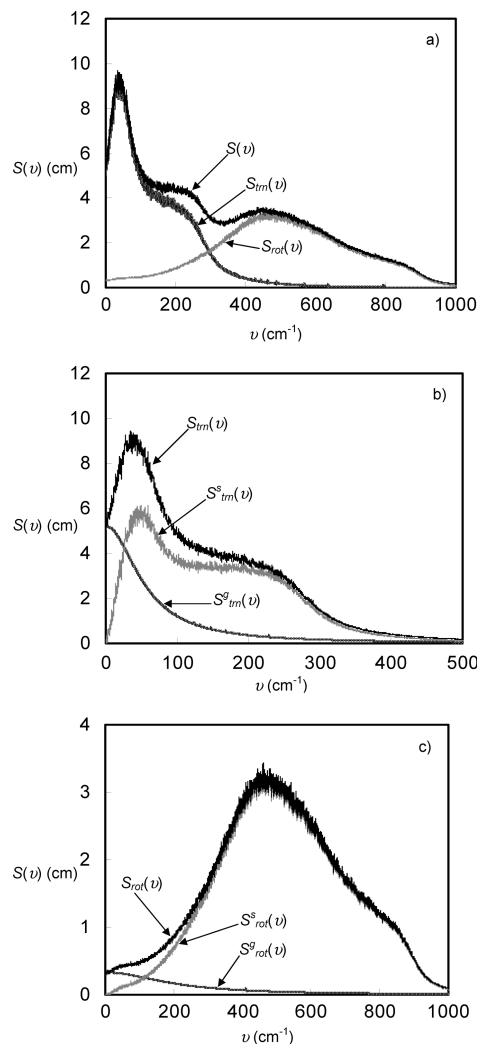


Figure 1. Density of state functions for liquid water (SPC model) at 25 °C and 1 g/cm³. (a) Total density of state function $S(v)$ and the translation $S_{trn}(v)$ and rotation $S_{rot}(v)$ components. (b) Translation density of state function and the gas $S_{g,trn}^g(v)$ and solid-like $S_{s,trn}^s(v)$ components. (c) Rotation density of state function $S_{rot}(v)$ and gas $S_{g,rot}^g(v)$ and solid-like $S_{s,rot}^s(v)$ components.

determined from eqs 23a, 24a, and 26 with the gas and harmonic weighting functions given in eqs 8a, 15a, and 25a.

TABLE 1: Comparison of Entropy (in Units of J/mol K) of Liquid Water at 25°C and 1 g/cm³ Calculated from the 2PT Method for Different Water Models

	water model				
	F3C	SPC	SPC/E	TIP3P	TIP4P-Ew
$S_{trn}(2PT)$	50.59 ± 0.25	53.05 ± 0.14	49.87 ± 0.14	55.59 ± 0.15	49.79 ± 0.07
$S_{rot}(2PT)$	11.54 ± 0.06	12.03 ± 0.03	10.41 ± 0.04	12.90 ± 0.04	9.53 ± 0.07
$S_{vib}(2PT)^a$	0.04 ± 0.00	-	-	-	-
$f_{trn}(2PT)^b$	0.25 ± 0.01	0.29 ± 0.01	0.23 ± 0.01	0.34 ± 0.00	0.24 ± 0.01
$f_{rot}(2PT)^b$	0.06 ± 0.00	0.07 ± 0.00	0.05 ± 0.00	0.08 ± 0.00	0.05 ± 0.00
$S(2PT)$	62.18 ± 0.30	65.09 ± 0.13	60.28 ± 0.16	68.49 ± 0.14	59.32 ± 0.12
$S(1PT)$	53.82 ± 0.13	56.24 ± 0.13	52.28 ± 0.18	59.37 ± 0.17	51.39 ± 0.09
$S(CT)^c$	-	70.10	66.60	72.70	66.30
$S(NN)^d$	-	73.51	66.91	80.19	65.46
$S(FD)^d$	-	65.10 ± 3.35	64.48 ± 3.35	70.86 ± 3.35	-
$S(FEP)^d$	-	68.20	63.36	72.58	63.62
$S(\text{expt})^e$	-	-	69.95 ± 0.03	-	-

^a SPC, SPC/E, TIP3P, and TIP4P-Ew are rigid water models and do not have vibration contributions. ^b Fluidicity factor in translation (f_{trn}) and rotational (f_{rot}) motions. ^c Data taken from the work of Henchman⁹ using the cell theory. ^d Data taken from the work of Wang et al.⁶ and Shirts and Pande²⁶ using the nearest-neighbors (NN) pair correlation function, the finite difference method (FD), and the free energy perturbation (FEP) method. ^e Experimental data are taken from the NIST database.²⁷

TABLE 2: Comparison of Energy and Entropy of SPC Water Determined with ($E(2PT)$) and $S(1PT)$) and without (E^{md} and $S(1PT)$) the 2PT method

T (K)	ρ (g/cm ³)	E^{md}	$E(2PT)$ (kJ/mol)	$E(\text{exptl})^a$	$S(1PT)$	$S(2PT)$ (J/mol K)	$S(\text{exptl})^a$	f_{tn} (–)	f_{rot} (–)
273.16	0.9998	–0.20	4.22	0.00	50.77	58.65	61.21	0.23	0.05
285.15	0.9993	0.80	4.97	0.91	53.57	62.23	65.40	0.28	0.06
298.15	0.9968	1.82	5.74	1.89	56.37	65.26	68.78	0.29	0.07
313.15	0.9925	2.98	6.66	3.02	59.66	68.77	72.60	0.32	0.07
333.15	0.9833	4.50	7.87	4.52	63.78	73.05	77.46	0.34	0.09
353.15	0.9718	5.98	9.08	6.03	68.14	77.35	82.31	0.39	0.09
373.15	0.9579	7.51	10.35	7.55	72.05	81.32	86.88	0.43	0.11
423.15	0.9166	11.18	13.50	11.38	81.55	90.35	96.42	0.48	0.13
473.15	0.8651	14.89	16.80	15.32	90.79	98.80	105.41	0.55	0.16
523.15	0.7994	18.79	20.34	19.46	99.78	107.11	113.44	0.58	0.18
573.15	0.7128	22.96	24.21	24.00	109.60	115.56	121.54	0.63	0.21
613.15	0.6105	27.02	28.02	28.28	118.45	123.51	128.49	0.66	0.24
633.15	0.5283	29.65	30.52	31.08	124.72	128.70	132.96	0.69	0.26
647.29	0.3170	35.09	35.73	36.57	138.61	139.21	141.63	0.77	0.32
633.15	0.1440	40.25	40.68	42.35	155.55	150.82	150.70	0.83	0.44
613.15	0.0926	42.03	42.39	44.35	163.88	155.76	154.85	0.87	0.51
573.15	0.0461	43.58	43.86	46.12	176.86	162.23	160.90	0.91	0.62
523.15	0.0199	44.52	44.73	46.89	193.24	168.55	167.33	0.95	0.75
473.15	0.0079	45.12	45.27	46.77	217.30	175.73	174.95	0.98	0.87
423.15	0.0025	45.15	45.23	46.10	239.04	184.71	184.50	0.99	0.95
373.15	5.98×10^{-4}	44.79	44.83	45.16	273.65	195.81	195.77	1.00	0.99
353.15	2.94×10^{-4}	44.54	44.56	44.71	280.67	202.37	202.35	1.00	0.99
333.15	1.30×10^{-4}	44.22	44.22	44.26	282.55	207.57	207.57	1.00	0.99
313.15	5.12×10^{-5}	43.76	43.76	43.78	297.85	214.01	213.86	1.00	0.99
298.15	2.31×10^{-5}	43.42	43.42	43.42	315.14	217.82	217.63	0.99	0.99
285.15	1.07×10^{-5}	43.10	43.10	43.09	310.91	222.85	222.85	0.99	0.99
273.16	4.85×10^{-6}	^b 42.80	^b 42.80	^b 42.80	306.14	227.89	227.89	0.99	0.99

^a Experimental data are taken from the steam table.²² ^b The reference state energy from MD is set so that simulation energies are the same as that from the steam table for saturated vapor at the triple point.

underestimate the entropy of water. The 2PT method correctly accounts the anharmonic effects for low frequency motions, with about 25% of the translational ($f_{\text{tn}} = 0.23$ to 0.34) and about 6% of the rotational ($f_{\text{rot}} = 0.05$ to 0.08) degrees-of-freedom being gas-like.

4.2. Entropy of Water along the Saturation Curve. A more stringent validation of the 2PT method is its applicability over a wide range of temperature and density. Table 2 summarizes the energy and entropy of SPC water simulated along the vapor–liquid saturation line from the triple point (273.16 K) to the critical point (647.29 K). At each temperature, both the liquid and the vapor phases are simulated using the density of real water (column 2 in Table 2). The comparison of entropy determined using the 1PT (harmonic approximation) and 2PT method is also illustrated in Figure 2. We see that the 2PT method provides reliable values of entropy for both the liquid and vapor water over the whole temperature ranges. The translational and rotational fluidicity (last two column in Table 2) varies from $f_{\text{tn}} = 0.23$ and $f_{\text{rot}} = 0.05$ at the triple point to $f_{\text{tn}} = 0.77$ and $f_{\text{rot}} = 0.32$ at the critical water, and $f_{\text{tn}} = f_{\text{rot}} = 1.0$ for densities and temperatures corresponding to gases (ideal gas state). This change in the fluidicity of water across the density range is consistent with our expectations. In contrast, the 1PT method underestimates entropy in the liquid phase and overestimates entropy in the vapor phase.

Also shown in Table 2 are the total energies of water along the saturation curve. The energies of SPC water (E^{md}) are in good agreement (about 2% error) with experiment. The difference between E^{md} and 2PT energy, $E(2PT)$, is the quantum correction and the zero point energy. The quantum corrections are negligible for gases but become significant for low temperature liquids.

Table 3 (and also in Figure 2) summarizes the 2PT entropy of saturated liquid water from the triple point to the critical

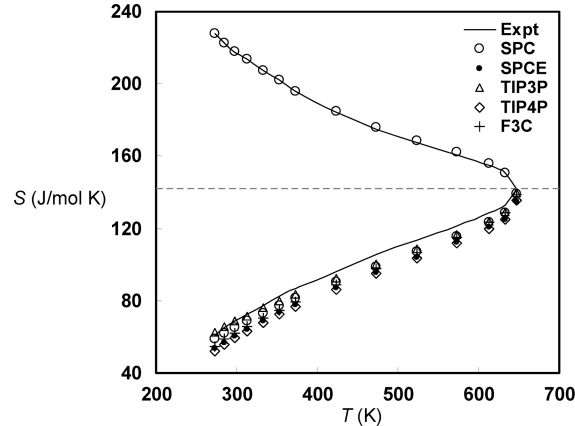


Figure 2. Entropy of liquid (below the dashed line) and vapor (above the dashed line) water along the vapor–liquid equilibrium curve (from triple point 273.16 K to the critical point 647.29 K) calculated using the 2PT method using different water models. The solid line represents experimental data. The dashed horizontal line indicates the entropy of water at the critical point.

point using five different water models. The difference in entropy from different models is largest at the triple point and is reduced at the critical point.

4.3. Convergence and Efficiency. A particularly attractive feature of the 2PT method is its fast convergence for entropy calculations. Figure 3 illustrates the standard deviation in the calculated entropy using trajectory of different lengths, 5, 10, 20, 50, 100, 200, and 500 ps after the system being equilibrated at 300 K. The entropy of liquid water converges after around 10–50 ps, whereas the convergence time is longer, about 200 ps, for vapor water. This is the time required for sufficient collisions between the gas molecules to obtain a converged

TABLE 3: Comparison of 2PT Entropy of Different Water Models for Saturated Liquids from the Triple Point to the Critical Point

T (K)	S(2PT) (J/mol K)				
	SPC	SPCE	TIP3P	TIP4P-Ew	F3C
273.15	58.65	53.54	62.76	51.99	54.79
285.15	62.23	56.82	65.57	55.59	58.74
298.15	65.26	60.54	68.64	59.23	62.11
313.15	68.77	64.15	71.68	63.08	65.62
333.15	73.05	68.95	76.03	68.01	70.46
353.15	77.35	73.41	79.93	72.58	74.81
373.15	81.32	77.54	83.66	76.66	79.22
423.15	90.35	87.15	92.48	86.42	88.88
473.15	98.80	95.88	100.57	95.21	97.69
523.15	107.11	104.26	108.71	103.60	106.53
573.15	115.56	112.66	116.67	112.14	115.26
613.15	123.51	120.59	124.17	119.78	123.27
633.15	128.70	125.18	129.36	125.06	128.65
647.15	139.21	135.19	139.73	135.64	138.55

density of state distribution. In practice, after equilibration of the MD for such times, an accurate value for the entropy can be obtained in ~ 10 ps. Thus, for practical calculations, the MD is run until the system is equilibrated, saving points along the trajectory every 1 ps, then the MD is continued for an additional 10 ps, keeping the trajectory every 4 fs. This decreases the issues of data storage.

The time evolution of the entropy of each individual water molecule can also be obtained from the 2PT method. Figure 4 illustrates the entropy population of water molecules from different lengths of simulation trajectories. At short times (e.g., 1 ps), the distribution is broad with many peaks. This indicates the presence of different chemical environments in the liquid phase. At longer times (e.g., 500 ps), each water may diffuse to sample the various environments, leading to a smooth Gaussian-type population distribution. The rapid convergence of the 2PT method and the capability of sampling entropy of individual molecules make it a powerful tool for studying the thermodynamics of water in biological systems. In particular, since the free energy can be obtained from just 10 ps of MD, the dynamical processes of such systems can be followed as they fold or react.

5. Conclusion

In this work, we extend the two-phase thermodynamic (2PT) model to describe molecular systems. We show that the 2PT

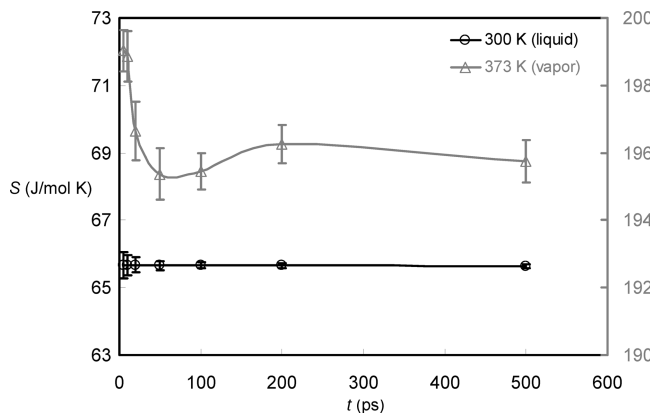


Figure 3. Entropy of SPC water determined based on different simulation times. The left axis is used for the liquid phase (300 K) simulations, and the right axis is used for the vapor phase simulations (373 K).

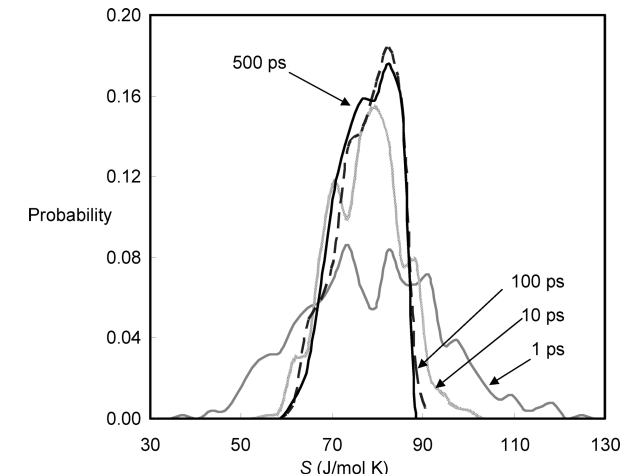


Figure 4. Time variation of the 2PT entropy population of water molecules at 300 K and 1 g/cm³. The distribution is determined from 512 water molecules, and its integration is unity.

method can produce converged entropies of liquid water from a short, 10 ps MD trajectory. We compare the entropy of water determined based on five water models, SPC, SPC/E, F3C, TIP3P, and TIP4P-Ew, and find that the 2PT entropy agrees well with more rigorous simulation techniques. We also show that the 2PT model is capable of producing the correct entropy of water in both the liquid and the vapor phases along the saturation curve from the triple point to the critical point. The rapid convergence and reliability of this method over a wide range of temperature and pressure (or density) conditions make it a practical tool to study the role of water in biological processes.

Acknowledgment. This research was partially supported by the National Science Council of Taiwan (NSC 98-2221-E-002-087-MY3) and the Ministry of Economic Affairs of Taiwan (98-5226904000-04-04). The computation resources from the National Center for High-Performance Computing of Taiwan and the Computing and Information Networking Center of the National Taiwan University are acknowledged.

References and Notes

- Jana, B.; Pal, S.; Maiti, P. K.; Lin, S. T.; Hynes, J. T.; Bagchi, B. *J. Phys. Chem. B* **2006**, *110*, 19611.
- Young, T.; Abel, R.; Kim, B.; Berne, B. J.; Friesner, R. A. *Proc. Natl. Acad. Sci. U.S.A.* **2007**, *104*, 808.
- White, R. P.; Meirovitch, H. *Proc. Natl. Acad. Sci. U.S.A.* **2004**, *101*, 9235.
- White, R. P.; Meirovitch, H. *J. Chem. Phys.* **2004**, *121*, 10889.
- Lazaridis, T.; Karplus, M. *J. Chem. Phys.* **1996**, *105*, 4294.
- Wang, L.; Abel, R.; Friesner, R. A.; Berne, B. J. *J. Chem. Theory Comput.* **2009**, *5*, 1462.
- Sharma, R.; Agarwal, M.; Chakravarty, C. *Mol. Phys.* **2008**, *106*, 1925.
- Tyka, M. D.; Sessions, R. B.; Clarke, A. R. *J. Phys. Chem. B* **2007**, *111*, 9571.
- Henchman, R. H. *J. Chem. Phys.* **2007**, *126*, 064504.
- Andricioaei, I.; Karplus, M. *J. Chem. Phys.* **2001**, *115*, 6289.
- Lin, S. T.; Blanco, M.; Goddard, W. A. *J. Chem. Phys.* **2003**, *119*, 11792.
- Zielkiewicz, J. *J. Chem. Phys.* **2008**, *128*, 196101.
- Berens, P. H.; Mackay, D. H. J.; White, G. M.; Wilson, K. R. *J. Chem. Phys.* **1983**, *79*, 2375.
- McQuarrie, A. A. *Statistical Mechanics*; Harper & Row: New York, 1976.
- Lin, S. T.; Maiti, P. K.; Goddard, W. A. *J. Phys. Chem. B* **2005**, *109*, 8663.
- Li, Y. Y.; Lin, S. T.; Goddard, W. A. *J. Am. Chem. Soc.* **2004**, *126*, 1872.

- (17) Levitt, M.; Hirshberg, M.; Sharon, R.; Laidig, K. E.; Daggett, V. *J. Phys. Chem. B* **1997**, *101*, 5051.
- (18) Jorgensen, W. L.; Chandrasekhar, J.; Madura, J. D.; Impey, R. W.; Klein, M. L. *J. Chem. Phys.* **1983**, *79*, 926.
- (19) Horn, H. W.; Swope, W. C.; Pitera, J. W.; Madura, J. D.; Dick, T. J.; Hura, G. L.; Head-Gordon, T. *J. Chem. Phys.* **2004**, *120*, 9665.
- (20) *Interaction Models for Water in Relation to Protein Hydration*; Berendsen, H. J. C., Postma, J. P. M., van Gunsteren, W. F., Hermans, J., Eds.; Reidel: Dordrecht, 1981; p 331.
- (21) Berendsen, H. J. C.; Grigera, J. R.; Straatsma, T. P. *J. Phys. Chem.* **1987**, *91*, 6269.
- (22) Van Wylen, G. J.; Sonntag, R. E. *Fundamentals of classical thermodynamics*, 2nd ed.; John Wiley & Sons: New York, 1978.
- (23) Plimpton, S. *J. Comput. Phys.* **1995**, *117*, 1.
- (24) Hockney, R. W.; Eastwood, J. W. *Computer Simulation Using Particles*; Taylor & Francis: New York, 1989.
- (25) Hoover, W. G. *Phys. Rev. A* **1985**, *31*, 1695.
- (26) Shirts, M. R.; Pande, V. S. *J. Chem. Phys.* **2005**, *122*, 134508.
- (27) NIST. Chemistry WebBook: Reference Database Number 69 ed.; National Institute of Standards and Technology, 2000.

JP103120Q